Archives of Hydro-Engineering and Environmental Mechanics
Vol. 51 (2004), No. 4, pp. 317–348

FE-Analysis of Patterning of Shear Zones in Granular Bodies for Earth Pressure Problems of a Retaining Wall

Jacek Tejchman

Gdańsk University of Technology, Civil Engineering Department,
ul. Narutowicza 11/12, 80-952 Gdańsk, Poland, e-mail: tejchmk@pg.gda.pl

(Received March 15, 2004; revised July 02, 2004)

Abstract

The evolution of shear zones in granular bodies for earth pressure problems of a retaining wall in conditions of plane strain was analyzed. The passive and active failure of a retaining wall was discussed. The calculations were carried out with a rigid and very rough retaining wall undergoing horizontal translation, rotation around the top and rotation around the bottom. The behaviour of dry sand was numerically modelled with a finite element method using a hypoplastic constitutive relation with polar extensions. Attention was paid to the influence of different wall movements on shear localization. The initial void ratio was assumed to be non-uniformly distributed. The geometry of calculated shear zones was compared with corresponding experimental results of laboratory model tests.

Key words: earth pressure, granular material, finite element method, hypoplasticity, polar continuum, retaining wall, shear localization

1. Introduction

The earth pressure on retaining walls belongs to the classical problems of soil mechanics. Despite intense theoretical and experimental research on this problem over more than 200 years, there remain considerable discrepancies between theoretical solutions and experimental results, due to the complexity of the deformation field in granular bodies near the wall caused by localization of deformations (which is a fundamental phenomenon of granular material behaviour). The localizations can appear as single, multiple or patterns of shear zones, depending upon initial and boundary conditions. They can be plane or curved. Within shear zones, pronounced grain rotations (Oda et al 1982, Uesugi et al 1988, Tejchman 1989, Geng et al 2003) and curvatures connected to couple stresses (Oda 1993), large strain gradients (Vardoulakis 1980), and high void ratios together with material softening (negative second-order work) (Desrues et al 1996) are observed.

The multiple patterns of shear zones are not usually taken into account in engineering calculations.

The realistic earth pressures can only be calculated with models which are able to describe the formation of shear zones with a certain thickness and spacing, i.e. the constitutive model must be endowed with a characteristic length of micro-structure. There are several approaches to capture spontaneous and induced shear localizations in granular bodies in a quasi-static regime: gradient (Aifantis 1984, Slyus 1992, de Borst et al 1992, Pamin 1994, Zervos et al 2001, Maier 2002, Tejchman 2004c), non-local (Bazant and Lin 1988, Brinkgreve 1994, Marcher and Vermeer 2001, Tejchman 2003, 2004a) and polar ones (Mühlhaus 1989, 1990, Tejchman 1989, de Borst 1991, Tejchman and Wu 1993, Steinmann 1995, Tejchman and Gudehus 2001). The approaches regularize the ill-posedness caused by strain-softening material behaviour and localization formation (differential equations of motion do not change their elliptic type during quasi-static calculations) (Mühlhaus 1989, de Borst et al 1992). Thus, the mesh-independent results are provided (Sluys 1992, Tejchman 1997). Otherwise, FE-results are completely controlled by the size and orientation of the mesh and thus produce unreliable results, i.e. the shear zones become narrower upon mesh refinement (element size becomes the characteristic length) and computed force-displacement curves change considerably depending on the thickness of the calculated shear zone (Brinkgreve 1994, Tejchman 1997).

The thickness of shear localizations depends on such various factors as: mean grain diameter (Vardoulakis 1980, Tejchman 1989, Tatsuoka et al 1991, 1994, 1997), pressure level (Tatsuoka et al 1991, Desrues and Hammad 1989), initial void ratio (Tejchman 1989, Desrues and Hammad 1989), direction of deformation (Tatsuoka et al 1994), grain roughness and grain size distribution (Tejchman 1989, Tatsuoka et al 1991, 1994). Thus, it is of a primary importance to use a constitutive model taking these into account.

In this paper, the capability of a polar hypoplastic constitutive model to describe the formation of the pattern of shear localization in granular bodies during a real geotechnical rate boundary value problem (passive and active earth pressure tests of a retaining wall), was demonstrated. The law takes into account the effect of initial density, pressure, deformation direction, mean grain size and grain roughness on the geometry of shear localization. The emphasis was focused upon the influence of the type of wall movements on the geometry of shear zones in sand with a non-uniform distribution of the initial void ratio. Only the plane strain case was taken into account. In the first step, the FE-calculations were performed with the same specimen size, granular material, wall height and wall roughness, and distribution of the initial void ratio. The calculated geometry of shear localization was qualitatively compared with results of some model tests. In turn, the computed earth pressure coefficients were compared with geotechnical formulas applied in practice and based on slip surfaces.

2. Literature Review

Coulomb (1775) indicated for the first time, the occurrence of shear zones during earth pressure tests. Darwin (1883) illustrated, with model tests, that the explanation of the behaviour of granular bodies during earth pressure is not possible without taking into account shear localization and procedure of filling (called by him a "historical effect"). Comprehensive experimental studies on earth pressure in sand were carried out at the Cambridge University between 1962 and 1974. During this period, a number of researchers (Arthur 1962, James 1965, Lucia 1966, May 1967, Bransby 1968, Adeosun 1968, Lord 1969, Smith 1972 and Milligan 1974) carried out experiments on the active and passive failure of a mass of dry sand deforming under plane strain conditions. The type of wall movement (passive wall translation (Lucia 1966), active wall rotation about its top (Lord 1969), passive wall rotation about its top (Arthur 1962, James 1965, Lord 1969), active wall rotation about its toe (Smith 1972, Milligan 1974), passive wall rotation about its toe (Bransby 1968, Adeosun 1968), wall height (0.152 m and 0.33 m), wall roughness (smooth and rough (James 1965, Milligan 1974)), wall flexibility (rigid wall and flexible wall (Milligan 1974)), initial density of sand (dense and loose (James 1965, Lord 1969)) and surcharge, were varied. In the case of a small earth pressure apparatus (Arthur 1962), the wall was 152 mm high and 152 mm wide. In the remaining cases, a large earth pressure apparatus, the retaining wall was 330 mm high and 190 mm wide. The dimensions of the sand specimen behind the wall were: 346 mm (height), 382 mm (length) and 200 mm (width) in a small apparatus, and 1500 mm (height) 1420 mm (length) and 195 mm (width) in a large apparatus. Generally, sand was poured at a different height from a moving hopper when the wall was fixed. In addition, dredged and back-filled experiments were carried out (Milligan 1974). In the first case, sand on one side of the wall was successfully removed. In the second case, the wall was partially embedded in sand and filling was continued on one side. In addition, the tests on soil cutting with an inclined wall were carried out (Bransby 1968, Adeosun 1968). The sand used was a rounded coarse quartz "Leighton Buzzard" sand (maximum void ratio 0.70, minimum void ratio 0.51, grain size between 0.6–1.2 mm, mean grain diameter 0.6 mm). The evolution of shear localization in sand was recognised using the radiographic technique which is able to detect density changes. Different modes of shear zones have been observed during passive and active earth pressure tests depending mainly on the type of the wall motion and surcharge. In passive tests with rigid walls rotating about the top, one or two curved shear zones were obtained in sand. Multiple curved shear zones of a similar shape were observed during tests with a wall rotating about the bottom. They occurred at the wall top and propagated towards the free boundary. During tests with a translating rigid wall, one slightly curved shear zone starting to form from the wall bottom, and secondary radial shear zones beginning at the wall top appeared. In active tests

with rigid walls, nearly parallel straight zones or a mesh of intersecting parallel zones close to the wall (wall rotating around the bottom) or a single curved zone (wall rotating around the top) were observed. The details of the tests at the Cambridge University and radiographs from Cambridge Archives of Radiographs were recently given by Leśniewska (2000).

Experimental studies of passive earth pressure on a retaining wall in sand were also conducted at Karlsruhe University by Gudehus (1986), and Gudehus and Schwing (1986). In these experiments, the wall was $h = 0.15$ m or $h = 0.20$ m high. In the case of $h = 0.20$ m, the dimensions of the sand specimen were: 570 mm (height), 630 mm (length) and 200 mm (width). In turn, in the case of $h = 0.15$ m, the dimensions of the sand specimen were: 200 mm (height), 400 mm (length) and 200 mm (width). The material used was "Karlsruhe" sand (maximum void ratio 0.84, minimum void ratio 0.53, grain size between 0.08–1.8 mm, mean grain diameter 0.45 mm). During a passive wall translation, one observed in dense sand a pattern of shear zones consisting of one major slightly curved shear zone starting to form at the wall toe and propagating towards the free boundary, radial zones linking the wall top and the curved shear zone and one shear zone parallel to the bottom of the sand body.

Earth pressures on a retaining wall are calculated within a theory of elasticity and plasticity. Within plastic limit states, there are generally two approaches: static and kinematic. In a first approach, assuming the material yielding behind the wall (according to the Mohr-Coulomb law), one can obtain mathematically closed solutions of pressures for simple boundary conditions (Caquot and Kerisel 1948, Negre 1959, Dembicki 1979) or numerical solutions using a method of stress and velocity characteristics by Sokolovski (1965) for cases with complex boundary and load conditions (Roscoe 1970, James and Bransby 1971, Szczepiński 1974, Bransby and Milligan 1975, Houlsby and Wroth 1982, Milligan 1983). In turn, within a kinematic approach, different failure mechanisms consisting of slip surfaces are assumed. From the equilibrium of forces on sliding wedges, a resultant total earth pressure is calculated (Coulomb 1775, Terzaghi 1951, Gudehus 1978, Wang 2000, Leśniewska and Mróz 2000). All theoretical solutions are very sensitive to internal friction and wall friction angles. They are not able to predict consistently deformations observed in experiments.

Finite element calculations are more realistic than analytical solutions since first, they take into account advanced constitutive laws describing the behaviour of granular material and second, they can predict the evolution of localization of deformation. For FE-analyses of earth pressures in granular soils, perfect plastic (Nakai 1985), a elasto-plastic (Simpson 1972, Simpson and Wroth 1974, Christian et al 1977, Potts and Fourie 1984, Fourie and Potts 1989, Leśniewska and Mróz 2003), elasto-plastic with remeshing (Hicks et al 2001), hypoplastic (Ziegler 1986), and polar hypoplastic constitutive law (Tejchman and Dembicki 2001, Tejchman 2002b, Nübel 2002) were used. A characteristic length of micro-structure was not

taken into account in the analyses except of calculations with a polar hypoplastic law. A pattern of shear zones calculated by Nübel (2002) for the case of an active dredged test with flexible walls was in accordance with experiments (Milligan 1974). In this analysis, a fluctuation of the initial void ratio with exponential distribution was attributed to the granular body. The numerical calculations by Leśniwska and Mróz (2001, 2003) revealed that the pattern of shear zones was easier to observe when a non-associated Coulomb-Mohr model without dilatancy was assumed. A FE-study carried out by Tejchman (2002a) with an uniform distribution of the initial void ratio in sand showed that the calculated deformation field with a wall rotating around the bottom (passive and active case) was different from the experimental one (Bransby 1968, Smith 1972). In addition, this study showed that the geometry of calculated shear zones was influenced by the size of the sand specimen and its initial void ratio. The pattern of induced shear zones was created also in the case of loose sand continuously subject to contractancy.

3. Constitutive Law

The FE-calculations were carried out adopting a hypoplastic law with polar extensions (Tejchman et al 1999, Tejchman and Gudehus 2001, Tejchman 2002a, Huang et al 2002, Nübel 2002, Gudehus and Nübel 2004, Nübel and Huang 2004) to describe shear localization.

Non-polar hypoplastic constitutive laws (Gudehus 1996a, Bauer 1996, von Wolffersdorff 1996) are an alternative to elasto-plastic formulations for continuum modelling of granular materials. They describe the evolution of effective stress components with the evolution of strain components by a differential equation including isotropic linear and non-linear tensorial functions according to the representation theorem by Wang (1970). They were formulated by heuristic process (starting from hypoelastic models) considering all requirements which seem to be important for granular material behaviour. In contrast to elasto-plastic models, the decomposition of deformation components into elastic and plastic parts, yield surface, plastic potential, flow rule and hardening rule are not needed. The hypoplastic models describe the behaviour of so-called simple grain skeletons which are characterised by the following properties (Gudehus 1996a):

- the state is fully defined through skeleton pressure and the void ratio (inherent anisotropy of contact forces between grains is not considered and vanishing principal stresses are not allowed),
- deformation of the skeleton is due to grain rearrangements (e.g. small deformations $< 10^{-5}$ due to an elastic behaviour of grain contacts, are negligible),
- grains are permanent (abrasion and crushing are excluded in order to keep the granulometric properties unchanged),

- three various void ratios decreasing exponentially with pressure are distinguished (minimum, maximum and critical),
- the material manifests asymptotic behaviour for monotonous and cyclic shearing or SOM-states for proportional compression,
- rate effects are negligible,
- physico-chemical effects (capillary and osmotic pressure) and cementation of grain contacts are not taken into account.

The hypoplastic constitutive laws are of the rate type. Due to incremental non-linearity with the deformation rate, they are able describe both a non-linear stress-strain and volumetric behaviour of granular bodies during shearing up, to and after the peak, with a single tensorial equation. They include also: barotropy (dependence on pressure level), pycnotropy (dependence on density), dependence on the direction of deformation rate, dilatancy and contractancy during shearing with constant pressure, increase and release of pressure during shearing with constant volume, and material softening during shearing of a dense material. They are apt to describe stationary states, i.e. states in which a grain aggregate can be deformed continuously at constant stress and constant volume under a certain rate of deformation. Although, hypoplastic models are developed without recourse to concepts of the theory of plasticity, failure surface, flow rule and plastic potential are obtained as natural outcomes (Wu and Niemunis 1996). The feature of the model is a simple formulation and procedure for determination of material parameters with standard laboratory experiments. The parameters are related to granulometric properties encompassing grain size distribution curve, shape, angularity and hardness of grains (Herle 1998, Herle and Gudehus 1999). Owing to that, one set of material parameters is valid within a large range of pressures and densities.

The disadvantage of a hypoplastic model is that it cannot realistically describe the behaviour of granulates upon cyclic loading. In this case, so-called ratcheting can be avoided by introducing an elastic domain in the hypoplastic laws with the aid of the intergranular strain of the interface layer between grains (Niemunis and Herle 1997). Due to the lack of an explicit yield surface, a sub-stepping iteration algorithm has to be used to avoid inadmissible stresses (Tejchman 1997). In addition, a hypoplastic constitutive law cannot describe realistically shear localization since it does not include a characteristic length. To take into account a characteristic length, polar terms were introduced with the aid of a polar (Cosserat) theory. The polar extension of the hypoplastic law was achieved analogously to a polar elasto-plastic formulation (Mühlhaus 1989).

The Cosserat theory takes into account two linked levels of deformation: micro-deformation at the micro-structure (particle) level and macro-deformation at the structural (continuum) level where the material is considered homogeneous (Schäfer 1962). Each material point has, for the case of plane strain or

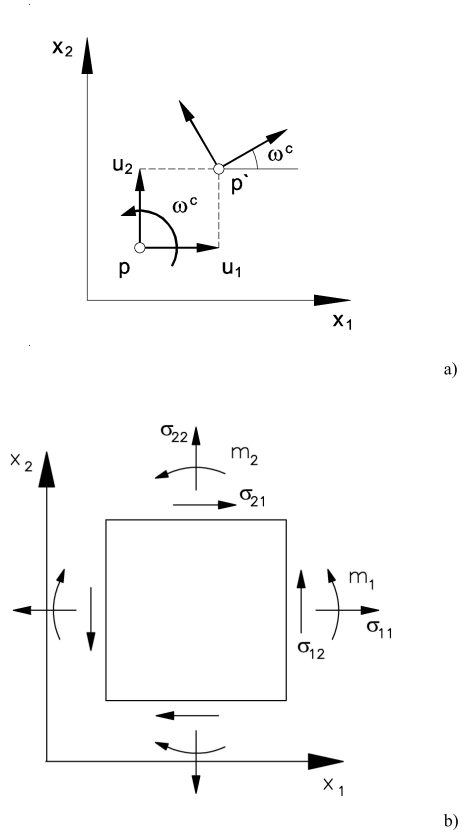

Fig. 1. Plane strain Cosserat continuum: a) degrees of freedom (u_1 – horizontal displacement, u_2 – vertical displacement, ω^c – Cosserat rotation), b) stresses σ_{ij} and couple stresses m_i at an element

axial-symmetric three degrees of freedom: two translational degrees of freedom and one independent rotational degree of freedom (Fig. 1a). The gradients of the rotation are connected to curvatures which are associated with couple stresses (Fig. 1b). This leads to non-symmetry of the stress tensor and the presence of a characteristic length. A polar approach is more suitable to model shear zones in granulates, as compared with other regularization techniques able to capture localization in a proper manner on better physical grounds, since it takes into account rotations and couple stresses which are observed during shearing, but remain negligible during homogeneous deformation (Oda 1993). Its other advantages are: the characteristic length is directly related to the mean grain diameter and a realistic wall boundary condition at interface of granulate with a structure can be derived (Tejchman 1997). Pasternak and Mühlhaus (2001) have demonstrated that the additional rotational degree of freedom of a Cosserat continuum arises naturally by mathematical homogenisation of an originally discrete system of spherical grains with contact forces and contact moments. Ehlers et al (2003) have recently shown

that a particle ensemble has the character of a micro-polar Cosserat continuum; the couple stresses naturally resulted only from the eccentricities of the normal contact forces.

In a polar hypoplasticity, stress and couple stress changes are described by two equations (Eqs. 1 and 2) of the rate type (Tejchman and Gudehus 2001, Tejchman 2002a, Tejchman and Bauer 2004):

$$\overset{o}{\sigma}_{ij} = f_s \left[L_{ij} \left(\hat{\sigma}_{kl}, \hat{m}_k, d^c_{kl}, k_k d_{50} \right) + f_d N_{ij} \left(\hat{\sigma}_{ij} \right) \sqrt{d^c_{kl} d^c_{kl} + k_k k_k d^2_{50}} \right], \tag{1}$$

$$\overset{o}{m}_i / d_{50} = f_s \left[L^c_i \left(\hat{\sigma}_{kl}, \hat{m}_k, d^c_{kl}, k_k d_{50} \right) + f_d N^c_i \left(\hat{m}_i \right) \sqrt{d^c_{kl} d^c_{kl} + k_k k_k d^2_{50}} \right], \tag{2}$$

$$\begin{aligned} L_{ij} &= a_1^2 d^c_{ij} + \hat{\sigma}_{ij} \left(\hat{\sigma}_{kl} d^c_{kl} + \hat{m}_k k_k d_{50} \right), \\ L^c_i &= a_1^2 k_i d_{50} + a_1^2 \hat{m}_i \left(\hat{\sigma}_{kl} d^c_{kl} + \hat{m}_k k_k d_{50} \right), \end{aligned} \tag{3}$$

$$N_{ij} = a_1 \left(\hat{\sigma}_{ij} + \hat{\sigma}^*_{ij} \right), \quad N^c_i = a_1^2 a_c \hat{m}_i, \tag{4}$$

$$\overset{o}{\sigma}_{ij} = \dot{\sigma}_{ij} - w_{ik}\sigma_{kj} + \sigma_{ik} w_{kj}, \quad \overset{o}{m}_i = \dot{m}_i - 0.5 w_{ik} m_k + 0.5 m_k w_{ki}, \tag{5}$$

$$d^c_{ij} = d_{ij} + w_{ij} - w^c_{ij}, \quad k_i = w^c_{,i}, \quad w^c_{kk} = 0, \quad w^c_{21} = -w^c_{12} = w^c = \dot{\omega}^c, \tag{6}$$

$$d_{ij} = 0.5 \left(v_{i,j} + v_{j,i} \right), \quad w_{ij} = 0.5 \left(v_{i,j} - v_{j,i} \right), \tag{7}$$

$$\overset{\bullet}{e} = (1 + e)\, d_{kk}, \tag{8}$$

$$\hat{\sigma}_{ij} = \frac{\sigma_{ij}}{\sigma_{kk}}, \quad \hat{m}_i = \frac{m_i}{\sigma_{kk} d_{50}}, \tag{9}$$

$$\begin{aligned} f_s &= \frac{h_s}{n h_i} \left(\frac{1 + e_i}{e} \right) \left(- \frac{\sigma_{kk}}{h_s} \right)^{1-n}, \\ h_i &= \frac{1}{c_1^2} + \frac{1}{3} - \left(\frac{e_{i0} - e_{d0}}{e_{c0} - e_{d0}} \right)^{\alpha} \frac{1}{c_1 \sqrt{3}}, \end{aligned} \tag{10}$$

$$f_d = \left(\frac{e - e_d}{e_c - e_d} \right)^{\alpha}, \tag{11}$$

$$e_i = e_{i0} \exp\left[-\left(-\sigma_{kk}/h_s\right)^n\right], \tag{12}$$

$$e_d = e_{d0} \exp\left[-\left(-\sigma_{kk}/h_s\right)^n\right], \tag{13}$$

$$e_c = e_{c0} \exp\left[-\left(-\sigma_{kk}/h_s\right)^n\right], \tag{14}$$

$$a_1^{-1} = c_1 + c_2\sqrt{\hat{\sigma}^*_{kl}\hat{\sigma}^*_{lk}}\left[1 + \cos(3\theta)\right], \quad \cos(3\theta) = -\frac{\sqrt{6}}{\left[\hat{\sigma}^*_{kl}\hat{\sigma}^*_{kl}\right]^{1.5}}\left(\hat{\sigma}^*_{kl}\hat{\sigma}^*_{lm}\hat{\sigma}^*_{mk}\right), \tag{15}$$

$$c_1 = \sqrt{\frac{3}{8}}\frac{(3 - \sin\phi_c)}{\sin\phi_c}, \quad c_2 = \frac{3}{8}\frac{(3 + \sin\phi_c)}{\sin\phi_c}, \tag{16}$$

where: σ_{ij} – Cauchy stress tensor and m_i – Cauchy couple stress vector, e – void ratio, $\overset{o}{\sigma}_{ij}$ – Jaumann stress rate tensor, $\overset{o}{m}_i$ – Jaumann couple stress rate vector, d^c_{ij} – polar rate of deformation tensor, k_i – rate of curvature vector, $\hat{\sigma}_{ij}$ – normalized stress tensor, $\hat{m}_i$ – normalized couple stress vector, d_{ij} – non-polar rate of deformation, w_{ij} – non-polar spin tensor, w^c – rate of Cosserat rotation, $v_{i,j}$ – gradient of velocity, f_s – stiffness factor, f_d – density factor, h_s – granular hardness, θ – Lode angle, e_c – critical void ratio, e_d – minimum void ratio, e_i – maximum void ratio (Fig. 2), e_{i0} – maximum void ratio at pressure equal to zero, e_{d0} – minimum void ratio at pressure equal to zero, e_{c0} – critical void ratio at pressure equal to zero, ϕ_c – critical angle of internal friction during stationary flow, n – oedometric coefficient, α – pycnotropy coefficient, d_{50} – mean grain diameter, a_c – micro-polar constant.

The constitutive relationship requires 9 material constants: e_{i0}, e_{d0}, e_{c0}, ϕ_c, h_s, n, α, d_{50} and a_c for a granular specimen (with an uniform distribution of the initial void ratio). The FE-analyses were carried out with the following material constants (for so-called Karlsruhe sand): $e_{i0} = 1.3$, $e_{d0} = 0.51$, $e_{c0} = 0.82$, $\phi_c = 30^\circ$, $h_s = 190$ MPa, $n = 0.5$, $\alpha = 0.3$, $d_{50} = 0.5$ mm, and $a_c = a_1^{-1}$ (Bauer 1996). The coefficient a_1 lies usually between 4.5 and 3.7 (Tejchman et al 1999) and determines the shape of the stationary stress surface calculated with a hypoplastic model (Bauer 1996). The parameters h_s and n are estimated from a single oedometric compression test with an initially loose specimen; h_s reflects the slope of the curve in a semi-logarithmic representation and n its curvature (Fig. 3). The constant α is found from a triaxial test with a dense specimen; it reflects the height and position of the peak value of the stress-strain curve. The angle ϕ_c is determined from the angle of repose or measured in a triaxial test with a loose

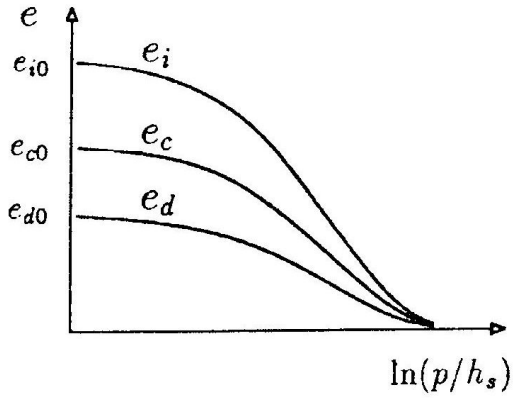

Fig. 2. Pressure dependence of void ratios

specimen. The values of e_{i0}, e_{d0}, e_{c0} and d_{50} are obtained with conventional index tests ($e_{c0} \approx e_{max}, e_{d0} \approx e_{min}, e_{i0} \approx (1.1 - 1.3) e_{max}$). The micro-polar constant a_c (which can be correlated with the grain roughness) was assumed on the basis of numerical calculations of shearing of an infinite narrow granular layer (Tejchman 1997). The smaller the constant, the greater the effect of Cosserat quantities on the material behaviour which is equivalent to the growth of the grain roughness.

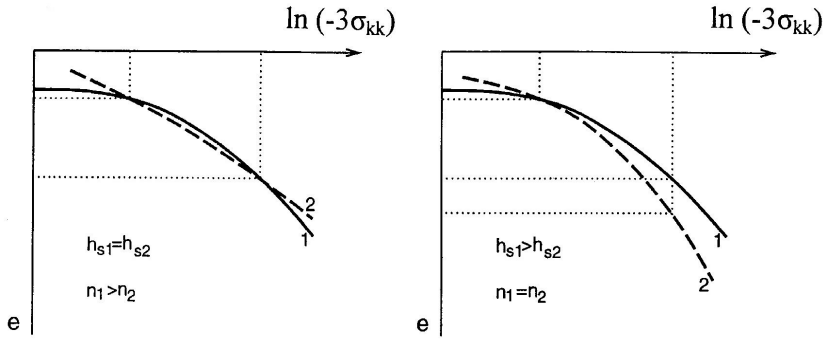

Fig. 3. Influence of coefficients n and h_s on compression curves for two different granular materials

The capability of polar hypoplastic constitutive laws has been already demonstrated in various boundary value problems involving localization such as biaxial compression (Tejchman 1997, 2002a, Tejchmn et al 1999, Nübel 2002, Maier 2002), monotonous and cyclic shearing of a narrow granular layer (Tejchman 2000, Tejchman and Gudehus 2001, Huang et al 2002, Tejchman and Bauer 2004), silo filling (Tejchman 1998), silo flow (Tejchman 2002c, Böhrnsen 2002), furnace flow (Zaimi 1998), footings (Tejchman and Herle 1999, Maier 2002, Nübel 2002) and sand anchors (Wehr and Tejchman 1999).

The characteristic length can be also taken into account within hypoplasticity by means of non-local terms (Maier 2002, Tejchman 2003, 2004a) or second gradient terms (Maier 2002, Tejchman 2004c).

4. Finite Element Implementation

The calculations were performed with a sand body of a height of H=200 mm and length of $L = 400$ mm (models test at the Karlsruhe University, Gudehus 1986, Gudehus and Schwing 1986). Quadrilateral finite elements composed of four diagonally crossed triangles were applied to avoid volumetric locking due to dilatancy effects (Groen 1997). Linear shape functions for displacements and the Cosserat rotation were used. In all, 3200 triangular elements were used. The height of the retaining wall located on the right side of the sand body was assumed to be $h = 170$ mm ($h/H = 0.85$). Integration was performed with three sampling points placed in the middle of each element side. The calculations were carried out with large deformations and curvatures (updated Lagrange formulation), changing the element configuration and the element volume. The initial stresses were generated using a K_o-state without polar quantities: $\sigma_{22} = \gamma x_2$, $\sigma_{11} = \sigma_{33} = K_0\ \gamma x_2$, $\sigma_{12} = \sigma_{21} = m_1 = m_2 = 0$ (σ_{11} – horizontal normal stress, σ_{22} – vertical normal stress, σ_{21} – horizontal shear stress, σ_{12} – vertical shear stress, m_1 – horizontal couple stress, m_2 – vertical couple stress (Fig. 1b), γ – initial volume weight of sand, x_2 – vertical coordinate measured from the top). The pressure coefficient at rest was assumed for dense sand to be $K_0 = 0.47$ on the basis of a so-called element test for oedometric compression (Herle 1998). Two sides and the bottom of the sand specimen were assumed to be very rough: $u_1 = 0$, $u_2 = 0$ and $\omega^c = 0$ (u_1 – horizontal displacement, u_2 – vertical displacement, ω^c – Cosserat rotation). The top of the sand specimen was traction and moment free. The retaining wall was assumed to be stiff and very rough ($u_2 = 0$ and $\omega^c = 0$). Three different wall modes were assumed in passive and active tests: uniform horizontal translation, rotation around the wall bottom and rotation around the wall top. The maximum horizontal displacement increments were chosen as $\Delta u/h = 0.00002$ (passive mode – wall moves against the backfill) and $\Delta u/h = 0.000004$ (active mode – wall moves away from the backfill)).

Since the numerical results of earth pressures by Tejchman (2002a) assuming a uniform distribution of the initial void ratio were different as compared with some experiments, the current calculations were carried out with a random distribution of the initial void ratio to enhance and promote the whole process of the shear zone formation. The non-homogenous distribution of void ratio is an inherent property of each granulate. The fluctuations of the initial void ratio are usually more marked for loose than for dense skeletons (Nübel 2002). The greater the fluctuations of void ratio, the greater are the stress changes (Behringer and Miller 1997, Geng et al 2003). In this FE-study, the initial void ratio e_o was

distributed non-uniformly in elements of the sand body by means of a random generator in such a way that the initial void ratio $e_0 = 0.60$ was increased in every element by the value $0.05 \times r$ ($e_o = 0.60 + 0.05r$), where r is a random number within the range of (0.01, 0.99). Thus, each element of the sand specimen had a different initial void ratio at the beginning of deformation. The assumed void ratio distribution was arbitrary to investigate only qualitatively the influence of an initially inhomogeneous state in a granular body on shear localization. Alternatively, the initial void ratio can be a distributed specimen with an exponential frequency function (Nübel and Karcher 1998, Nübel 2002, Tejchman 2004b).

For the solution of the non-linear equation system, a modified Newton-Raphson scheme with line search was used using an initial global stiffness matrix calculated with only two first terms of the constitutive equations (which are linear in d^c_{kl} and kd_{50}). To accelerate the calculations in the softening regime, the initial increments of displacements and the Cosserat rotation in each calculation step were assumed to be equal to the converged increments from the previous step (Vermeer and van Langen 1989, Tejchman 1989). The iteration steps were performed using translational and rotational convergence criteria. For the time integration of stresses and couple stresses in finite elements, a one-step Euler forward scheme was applied. To prevent eventual inadmissible stresses, a substepping algorithm was used (deformation and curvature increments were divided into small parts within each step). In addition, to avoid tensile stresses near the wall base (singular field) and along the free boundary a significantly smaller granular hardness h_s was assumed ($h_s = 0.19$ MPa). If tensile stresses were obtained in some elements at the wall base and along the free boundary, the stresses and couple stresses in these elements were replaced by values equal to zero.

5. Numerical Results (Passive Case)

The FE-results of a plane strain passive earth pressure problem for dense sand ($e_o = 0.60 + 0.05r$, $\gamma = 17.0$ kN/m^3) within a polar continuum are shown in Figs. 4–9. Figure 4 presents the evolution of the normalized horizontal earth pressure force $2E_h/(\gamma h^2)$ versus the normalized horizontal wall displacement u/h for three different wall movements. In the case of a rotating wall, the horizontal displacement u is related to the wall displacement of the bottom point (wall rotating about the top) or top point (wall rotating around the bottom). The force E_h was calculated as the integral of mean horizontal normal stresses σ_{11} from quadrilateral elements along the retaining wall. In Figs. 5–7, the deformed meshes with the distribution of the void ratio and Cosserat rotation in the residual state are shown. The darker region indicates the higher void ratio. The Cosserat rotation is marked by circles with a diameter corresponding to the magnitude of the rotation in the given step. The distribution of the Cosserat rotation at the beginning of the passive wall translation is described in Fig. 8. The distribution of Cosserat

rotation ω^c and void ratio e across the normalized initial specimen height x_2/d_{50} in two sections at $x_1 = 0.15$ m and $x_1 = 0.30$ m (measured from the left side) at residual state is presented in Fig. 9 (during passive wall translation). The positive Cosserat rotation corresponds to that of Fig. 1a.

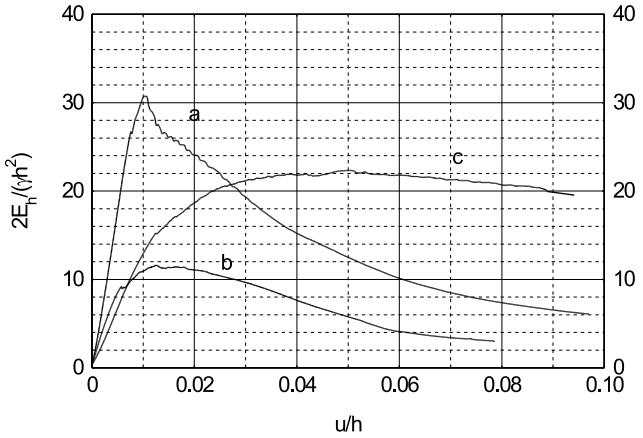

Fig. 4. Resultant normalized earth pressure force $2E_h$ (γh^2) versus normalized wall displacement u/h (passive case): a) translating wall, b) wall rotating around its top, c) wall rotating around its bottom

The evolution of curves of the horizontal earth pressure $2E_h$ /(γh^2) is similar in all three cases (Fig. 4). The forces increase, reach a maximum for about $u/h =$ 1–5%, next show softening and tend to asymptotic values for about $u/h =$ 7–9%. For the wall rotation about the bottom, a decrease of the curve is smaller (in the considered range of u/h). The maximum horizontal force on the wall is the highest for the wall translation, and the lowest for the wall rotation about the top. The maximum normalized horizontal earth pressure forces are high ($2E_h/\gamma h^2 =$ 12–31) due to the high initial void ratio of sand, large wall roughness, high relationship between the mean grain diameter and wall height and low initial stress level. The calculated minimum (residual) earth pressure coefficients are about 3.0–6.0 (Fig. 4).

Shear localization which is characterized in dense granulates among others by the appearance of the Cosserat rotation and a strong increase of the void ratio is strongly dependent upon the type of the wall mode (Figs. 5–7). For the wall translation (Figs. 5 and 9), five shear zones are obtained: one vertical along the very rough retaining wall, one zone projecting horizontally from the wall base, one inclined (slightly curved) zone spreading between the wall bottom and free boundary, and two radial oriented shear zones starting to form at the wall top. The inclined shear zone becomes dominant in the course of deformation. The horizontal shear zone develops only at the beginning of the wall translation

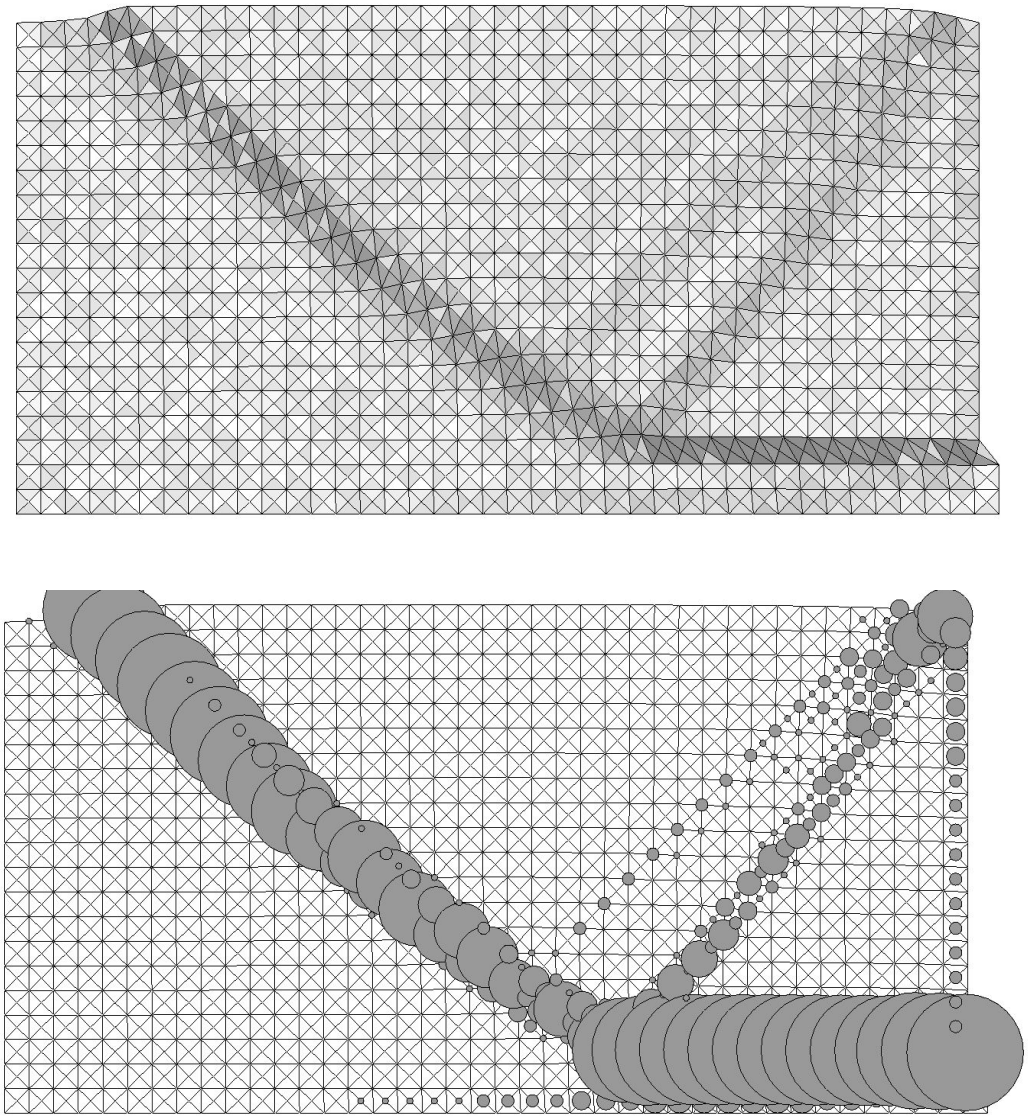

Fig. 5. Deformed FE-meshes with distribution of void ratio and Cosserat rotation for dense sand during passive earth pressure with translating wall ($u/h = 0.05$)

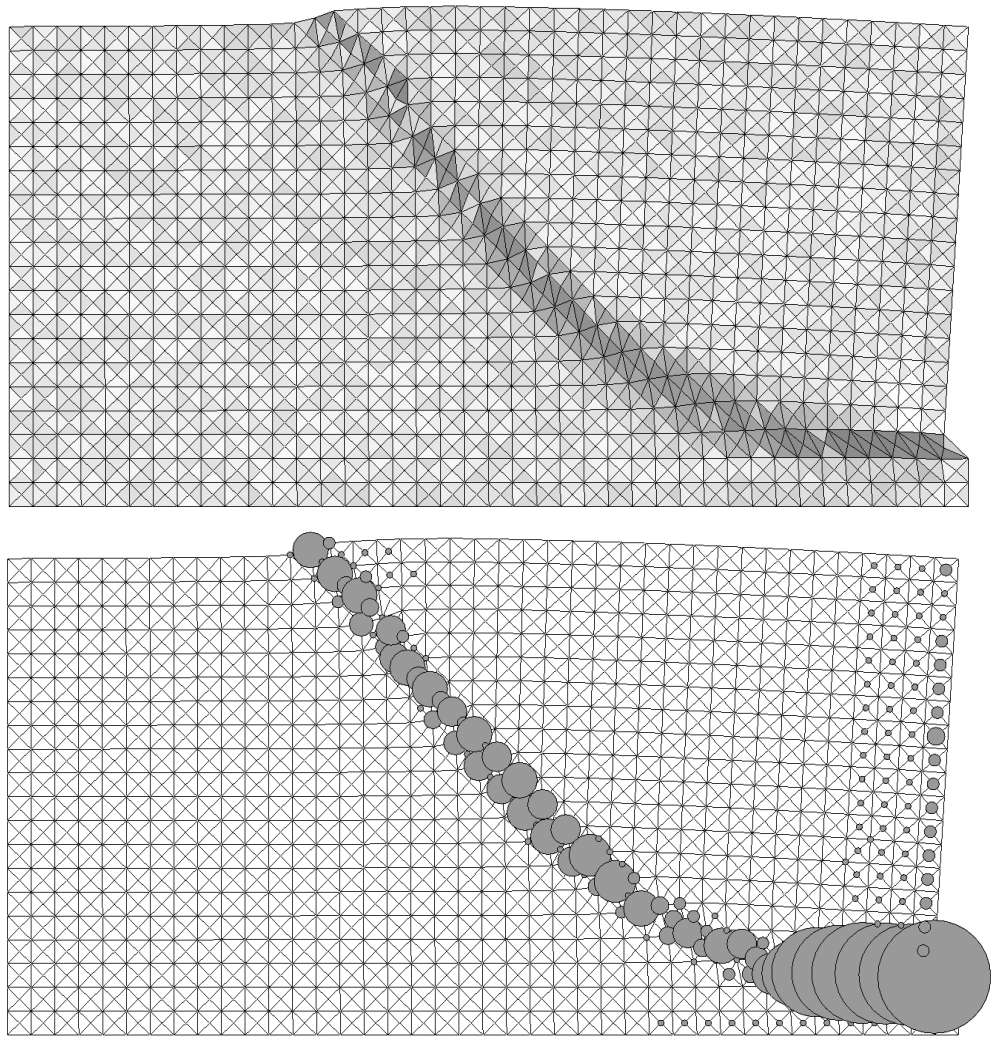

Fig. 6. Deformed FE-meshes with distribution of void ratio and Cosserat rotation for dense sand during passive earth pressure with wall rotating around its top ($u/h = 0.06$)

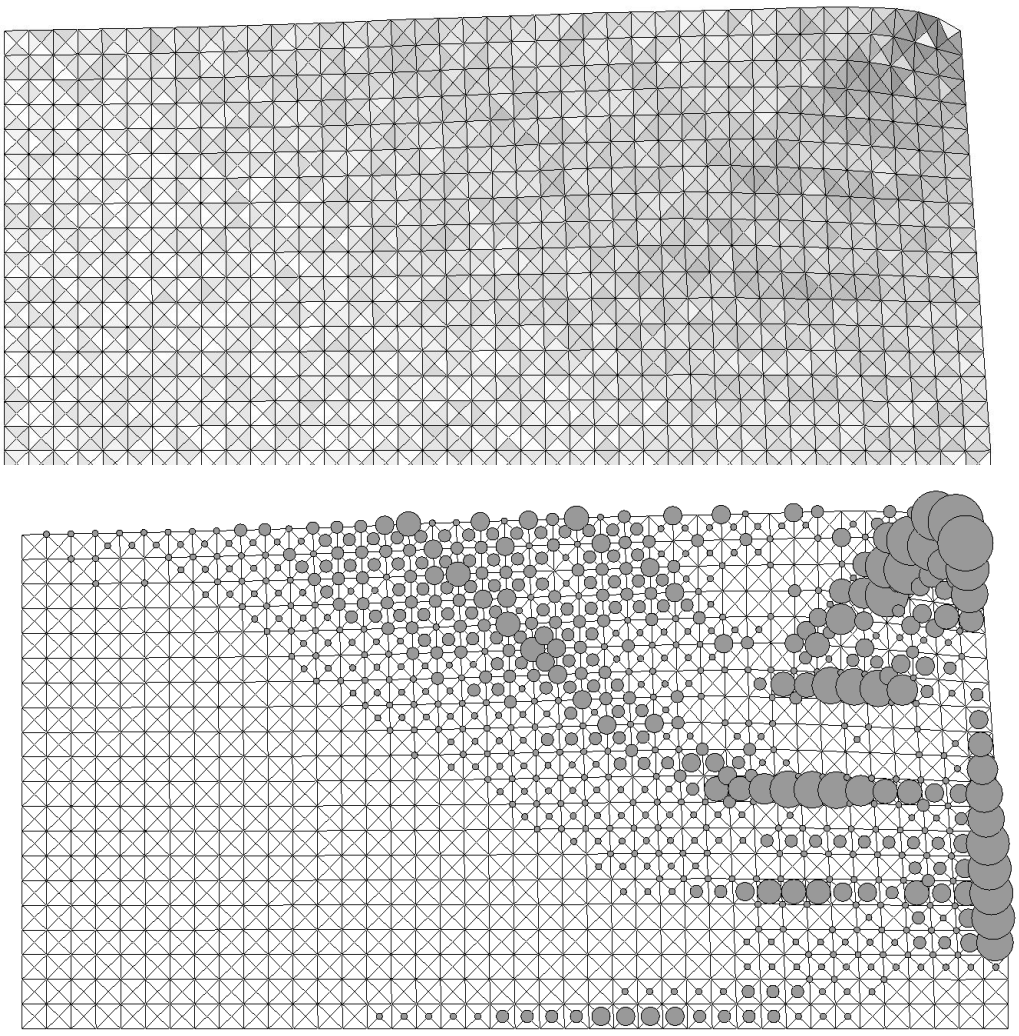

Fig. 7. Deformed FE-meshes with distribution of void ratio and Cosserat rotation for dense sand during passive earth pressure with wall rotating around its bottom (u/h=0.07)

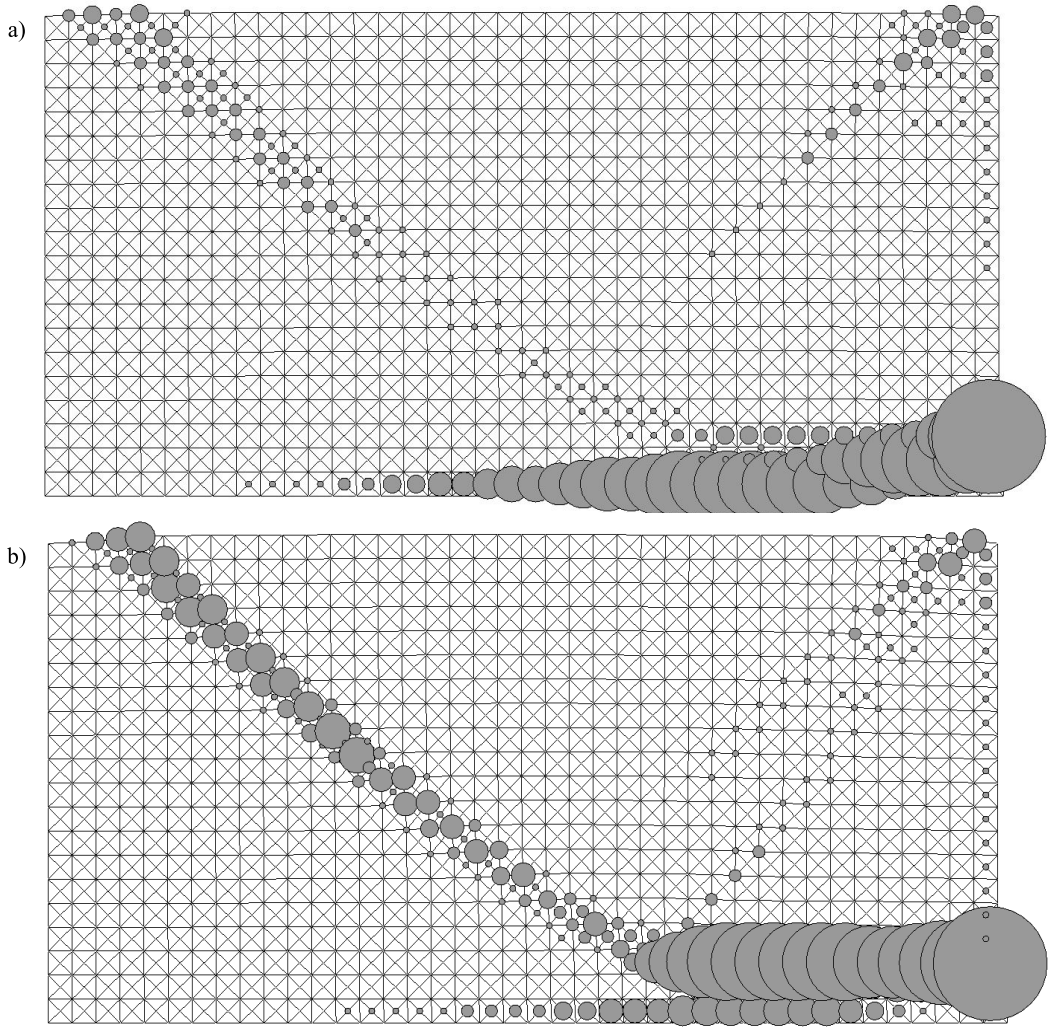

Fig. 8. Distribution of Cosserat rotation in dense sand at the beginning of passive earth pressure with translating wall: a) $u/h=0.01$, b) $u/h=0.02$

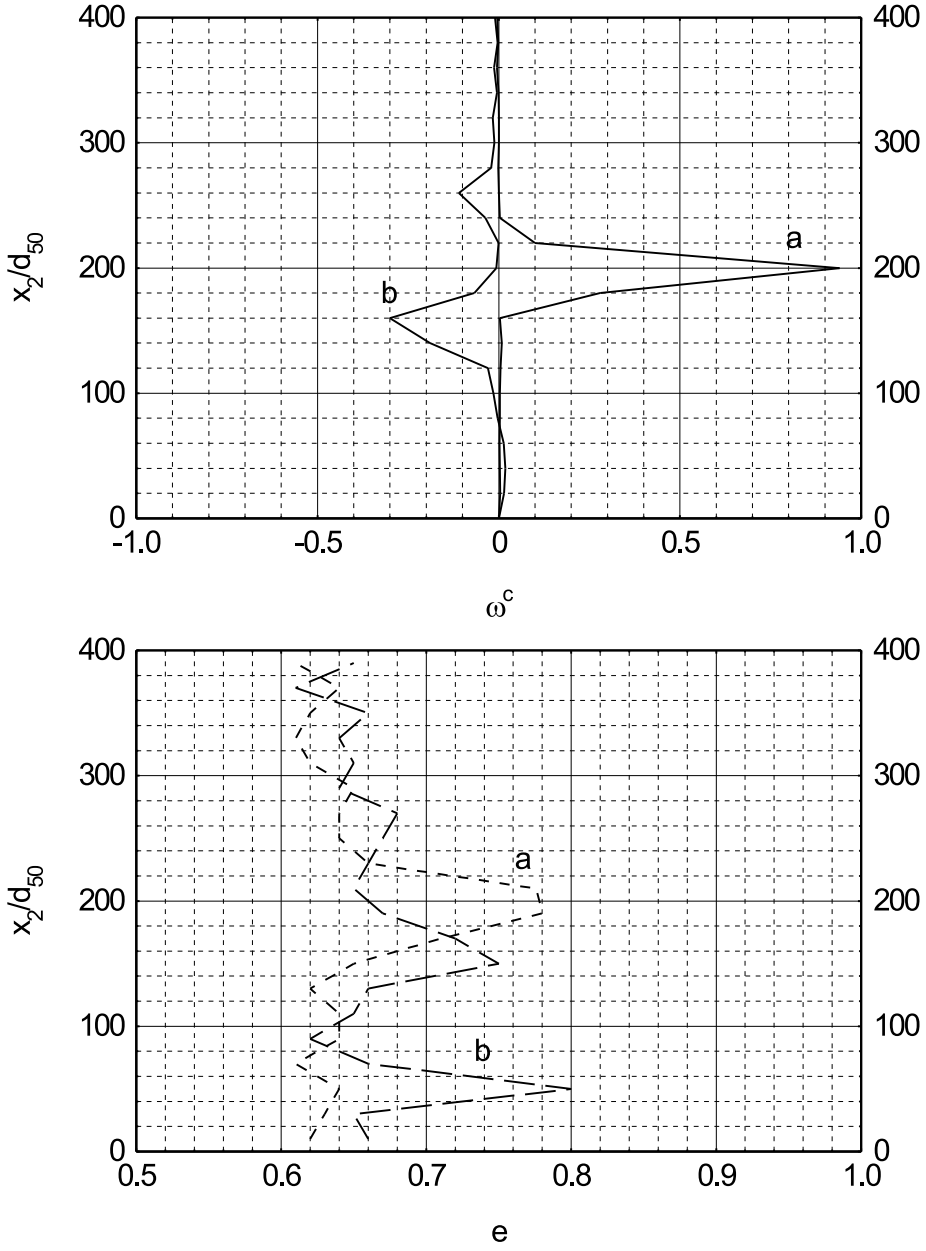

Fig. 9. Distribution of Cosserat rotation ω^c and void ratio e across the normalized specimen height x_2/d_{50} at residual state during passive earth pressure with translating wall ($u/h=0.08$): a) $x_1=0.0.15$ m, b) $x_1=0.30$ m

(Fig. 8). The material starts to generate the Cosserat rotation and to dilate at the same time at three different places (wall bottom, wall top and free boundary on the left side), Fig. 8. Next, the shear zone (starting from the wall base) curves upwards, becomes straight and reaches the free boundary. Later, it is approached by one radial shear zone. The second radial shear zone is not fully developed at $u/h = 0.07$. The thickness of the dominant shear zone is about $30 \times d_{50}$ (on the basis of the Cosserat rotation, Fig. 9) and its inclination from the bottom is about $\theta = 40^\circ$.

The values of void ratio e and mobilized internal friction angle ϕ in the middle of the shear zones are near the peak of the load-displacement curve (at $u/h = 0.01$): $e = 0.65$ and $\phi = 45.2^\circ$ (inclined zone at $x_1 = 0.05$ m), $e = 0.68$ and $\phi = 42.0^\circ$ (inclined zone at $x_1 = 0.10$ m), $e = 0.64$ and $\phi = 44.8^\circ$ (horizontal zone at $x_1 = 0.15$ m), $e = 0.63$ and $\phi = 48.8^\circ$ (lower radial zone at $x_1 = 0.15$ m), and $e = 0.63$ and $\phi = 48.1^\circ$ (upper radial zone at $x_1 = 0.15$ m). At the normalized horizontal displacement of $u/h = 0.08$, they are, respectively: $e = 0.79$ and $\phi = 34.6^\circ$ (inclined zone at $x_1 = 0.05$ m), $e = 0.78$ and $\phi = 35.0^\circ$ (inclined zone at x_1=0.10 m), $e = 0.80$ and ϕ=33.5° (horizontal zone at $x_1 = 0.15$ m), $e = 0.74$ and ϕ=37.2° (lower radial zone at $x_1 = 0.15$ m), and $e = 0.67$ and $\phi = 43.3^\circ$ (upper radial zone at $x_1 = 0.15$ m). The angles of internal friction were calculated from Mohr's formula

$$\phi = \arcsin \frac{\sigma_1 - \sigma_2}{\sigma_1 + \sigma_2}, \tag{17}$$

where the principle stresses $\sigma_{1,2}$ are (Schäfer 1962):

$$\sigma_{1,2} = \frac{\sigma_1 + \sigma_2}{2} \pm \sqrt{\left(\frac{\sigma_1 - \sigma_2}{2}\right)^2 + \left(\frac{\sigma_{12} + \sigma_{21}}{2}\right)^2}. \tag{18}$$

The largest void ratios in the inclined and horizontal shear zones at u/h=0.08 (calculated with Eq. 8) are equal to the pressure-dependent critical values e_c (Eq. 4), Fig. 9. The critical void ratios in the radial shear zones have not yet been obtained. Beyond the shear zones, the residual void ratio is equal to 0.61–0.65. The calculated geometry of shear zones is in agreement with experimental observations at Cambridge University by Lucia (1966) (Fig. 10a) and at Karlsruhe University by Gudehus (1986) and Gudehus and Schwing (1986) (Fig. 10b).

The maximum normalized horizontal earth pressure forces ($2E_h / \gamma h^2 = 12$–31) are in the range of the usual (engineering) earth pressure coefficients (Dembicki 1979, Gudehus 1996b) determined under the assumption of one circular slip line ($K_{pr} = 11.33$–25.80) and three straight slip lines ($K_{pt} = 13.40$–23.70) at $\delta = \varphi^p = 40^\circ$–$45^\circ$ (δ – wall friction angle, φ^p – internal friction angle of dense sand at peak). However, the actual friction angles at peak φ^p in the shear zones are not known in advance (they depend strongly on the initial and boundary conditions of

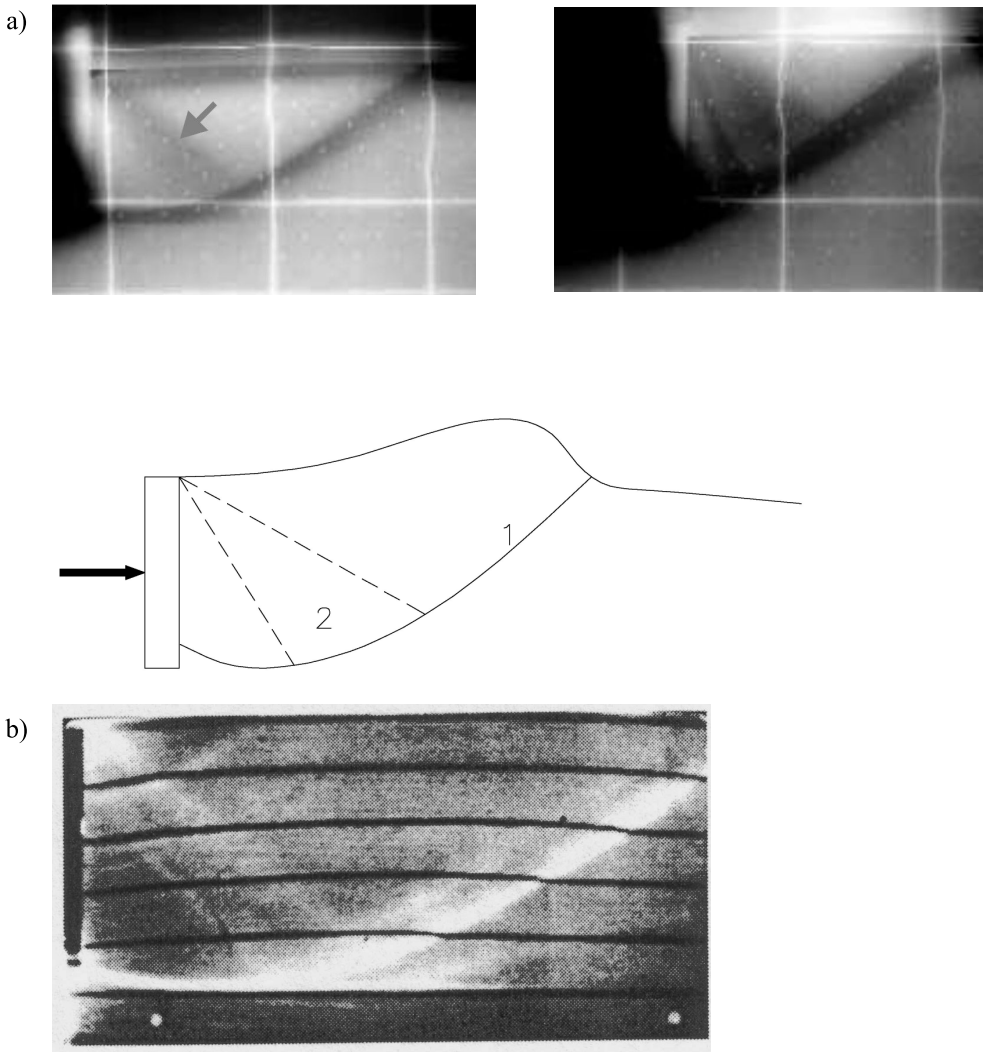

Fig. 10. Shear zones observed in experiments (radiograhs and schematically): a) during passive wall translation (Lucia 1966), b) during passive wall translation (Gudehus and Schwing 1986), c) during passive wall rotation around the top (Arthur 1962) and d) during passive wall rotation around the bottom (Bransby 1968) from Leśniewska (2000)

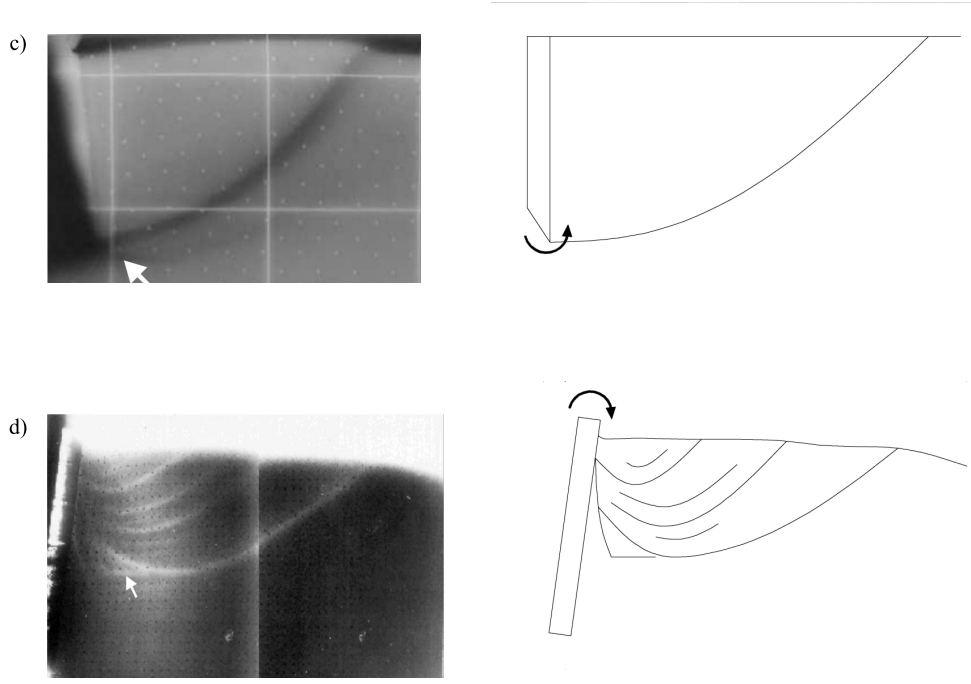

Fig. 10. Cont.

the entire system). It is therefore difficult to obtain realistic earth pressures with a conventional earth pressure theory. In addition (as the numerical calculations show), the different friction angles are mobilized in the various shear zones at the same time. The different friction angles occur also along the same shear zone.

In the case of wall rotation around the top (Fig. 6), only one shear zone occurs which is more curved than the shear zone during the wall translation. The calculated deformation field is close to the experimental one (Arthur 1962) (Fig. 10c).

When the retaining wall rotates around the bottom (Fig. 7), a pattern of curved parallel shear zones is obtained. This result is approximately in accordance with experiments (Bransby 1968) (Fig. 10d).

6. Numerical Results (Active Case)

The FE-results of a plane strain active earth pressure problem with a dense sand specimen are shown in Figs. 11–14. Figure 11 shows the evolution of the normalized horizontal earth pressure force $2E_h/(\gamma h^2)$ versus the normalized horizontal wall displacement u/h for three different wall movements in the case of dense sand ($e_o = 0.60 + 0.05r$, $\gamma = 17.0$ kN/m^3). In Figures 12–14, the deformed meshes

with the distribution of the void ratio and Cosserat rotation in the residual state are demonstrated.

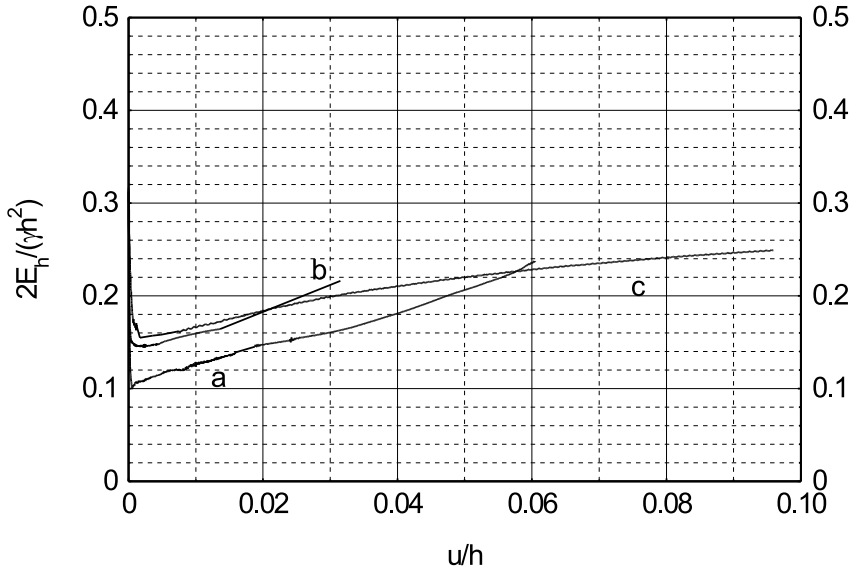

Fig. 11. Resultant normalized earth pressure force $2E_h\ /(\gamma h^2)$ versus normalized wall displacement u/h (active case): a) translating wall, b) wall rotating around its top, c) wall rotating around its bottom

All earth pressure curves drop sharply at the beginning of the wall movement, reach the minimum at $u/h = 0.001$–0.002 and next increase continuously (Fig. 11). For the case of a wall rotating around its bottom, the residual state was reached for $u/h = 0.1$. The lowest earth pressure force occurs with the wall translation, and the largest with the wall rotation about the top. Thus, the relationship between the minimum active earth pressure and the type of the wall movement is inversed as compared with the maximum passive earth pressure and type of wall movement. The minimum normalized earth pressure forces ($2E_h\ (\gamma h^2 = 0.10 - 0.16)$ are slightly less than the usual earth pressure coefficients (Gudehus 1996b) assuming a circular slip line ($K_a = 0.16$–0.20) or a straight slip line ($K_a = 0.14$–0.16) with $\delta = \varphi^p$ ($\varphi^p = 40^\circ$–45°).

The calculated pattern of shear zones depends again on the type of wall movement. In the case of wall translation, two pronounced shear zones are obtained (Fig. 12). A vertical one occurs along the wall, and the second one propagates from the wall bottom up to the free boundary. The internal shear zone is slightly curved with a mean inclination to the bottom of $\theta = 50^o$. The thickness of the shear zone is again about (30–35) $\times d_{50}$. This result is close to the experimental one (Szczepiński 1974).

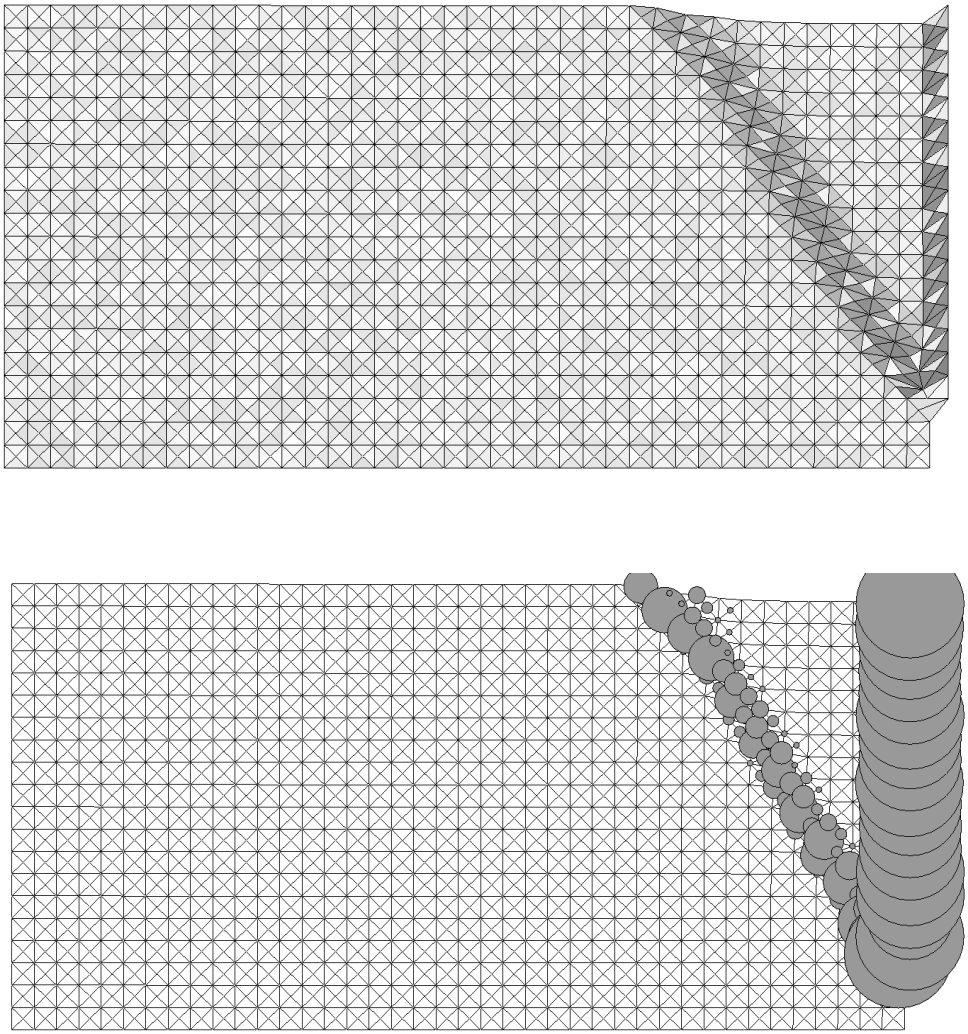

Fig. 12. Deformed FE-meshes with distribution of void ratio and Cosserat rotation for dense sand during active earth pressure with translating wall ($u/h=0.06$)

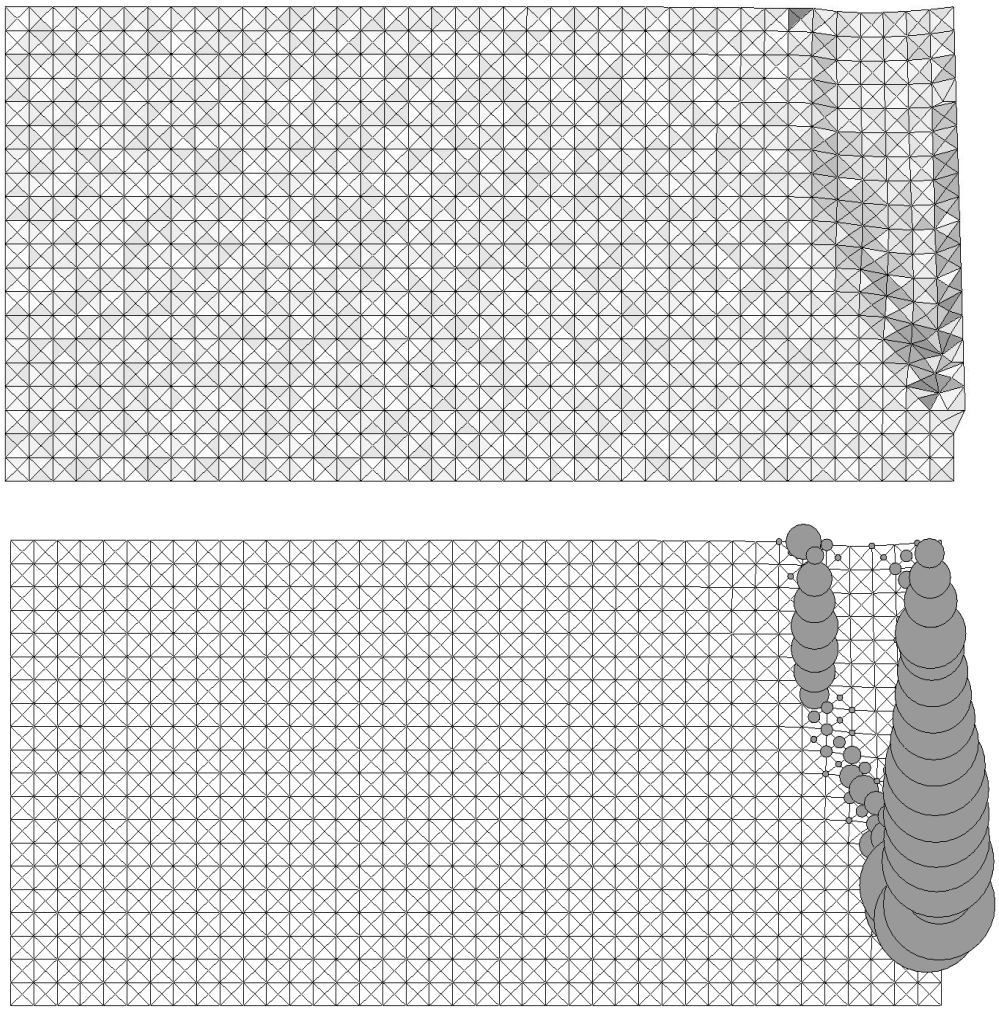

Fig. 13. Deformed FE-meshes with distribution of void ratio and Cosserat rotation for dense sand during active earth pressure with wall rotating around its top ($u/h=0.03$)

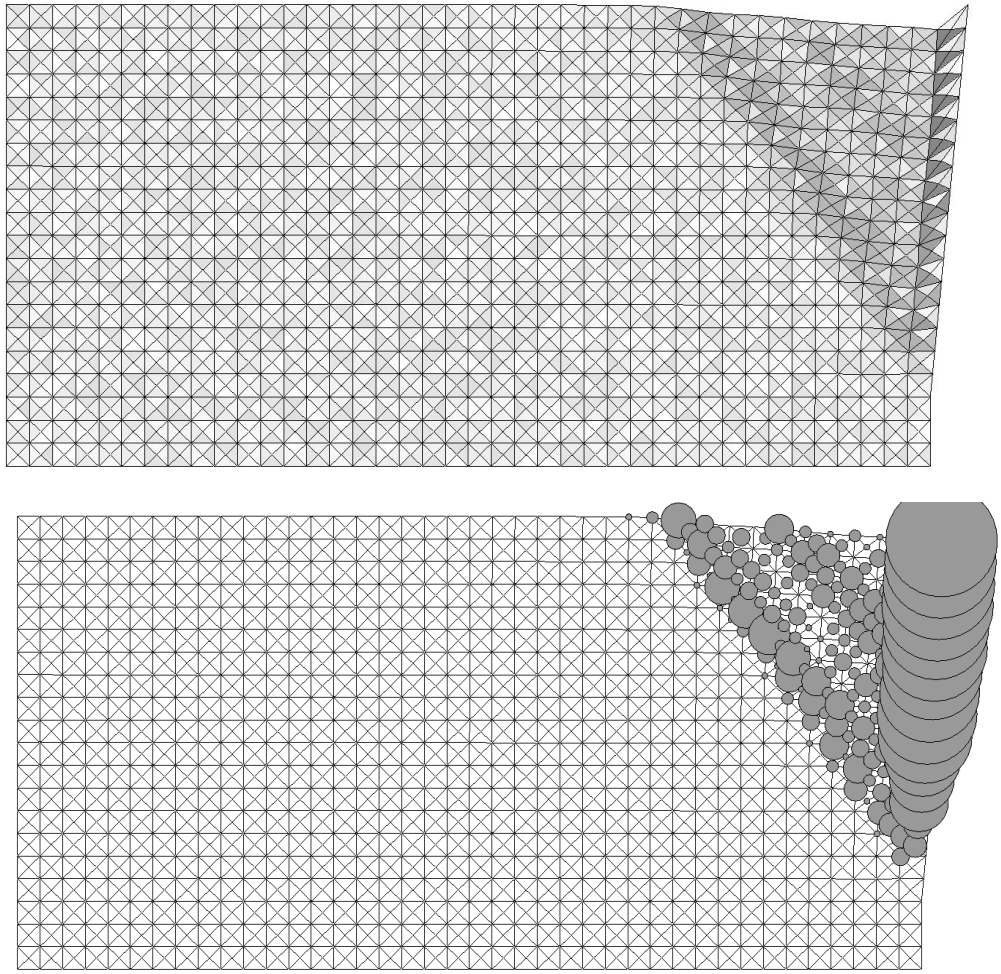

Fig. 14. Deformed FE-meshes with distribution of void ratio and Cosserat rotation for dense sand during active earth pressure with wall rotating around its bottom ($u/h=0.09$)

When the wall rotates around the top, two shear zones are obtained again: the first along the wall and the second inside sand starting from the wall bottom (Fig. 13). The shear zone is strongly curved. A similar result was obtained in the experiment (Lord 1969) (Fig. 15a).

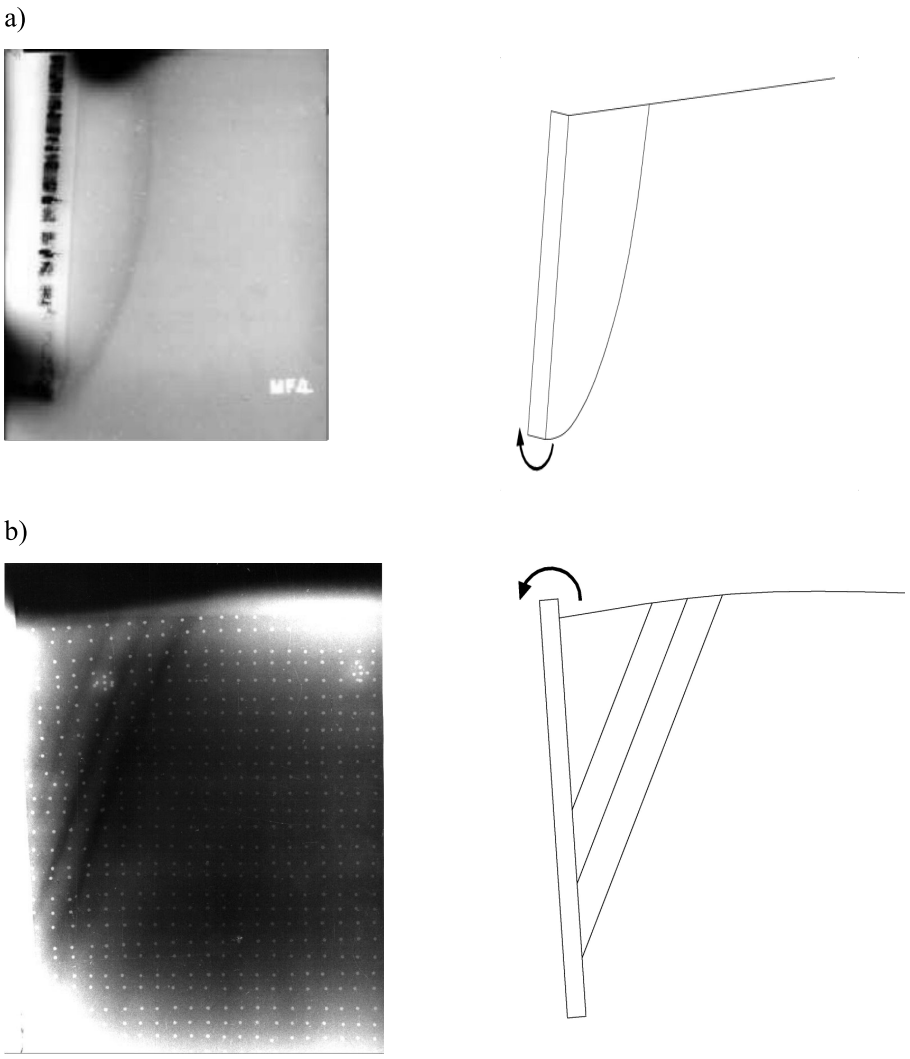

Fig. 15. Shear zones observed in experiments (radiograhs and schematically): a) during active wall rotation around the top (Lord 1969) and b) during active wall rotation around the bottom (Smith 1972) from Leśniewska (2000)

In the case of a wall rotating about the bottom (Fig. 14), three shear zones are obtained: one along the wall and two parallel internal. This is in accordance with the experiment (Smith 1972) (Fig. 15b).

7. Conclusions

The following conclusions can be drawn on the basis of the FE-studies performed on shear localization during plane strain earth pressure problems with very rough and rigid retaining walls:

- A polar hypoplastic approach is capable of capturing a complex patterning of shear zones in granular materials,
- The geometry of shear zones depends greatly on the direction and type of wall movement (passive or active, translation or rotation). The experimental deformation field was realistically reproduced.
- The effect of non-uniform distribution of the initial void ratio on the geometry of shear zones is of major importance in the case of passive and active wall rotation around the bottom.
- The largest passive earth pressures occur with the horizontal translation of the wall, they are smaller with wall rotation around the bottom and again smaller with wall rotation around the top. The smallest active earth pressures are created during wall translation, and the largest during wall rotation around the top.
- The granular material tends to a critical state inside shear zones. The Cosserat rotations are noticeable only in shear zones.
- The earth pressures significantly change with wall displacement.
- Conventional earth pressure mechanisms with slip surfaces are roughly reproduced. Realistic earth pressure coefficients can be obtained with actual values of internal friction angles.

Calculations will be continued with different specimen size, sand, wall roughness and wall stiffness. To compare numerical load-displacement curves with experimental ones, the FE-analyses will be performed strictly according to conditions of laboratory experiments. Different extended hypoplastic models including a characteristic length (polar, non-local and second gradient) will be compared. Later, a remeshing technique (Ehlers and Graf 2003) will be adopted to perform the analysis for large geotechnical problems.

References

Adeosun A. (1968), *Lateral Forces and Failure Patterns in the Cutting of Sands*, Research Project, University of Cambridge.

Aifantis E. C. (1984), On the Microstructural Origin of Certain Inelastic Models, *J. Eng. Mater. Technol.*, 106, 326–334.

Arthur J. R. F. (1962), *Strains and Lateral Force in Sand*, PhD Thesis, University of Cambridge.

Bauer E. (1996), Calibration of a Comprehensive Hypoplastic Model for Granular Materials, *Soils and Foundations*, 36, 1, 13–26.

Bazant Z., Lin F. B. (1988), Nonlocal Yield Limit Degradation, *Int. J. Num. Meth. Eng.*, 26, 1805–1823.

Behringer R. P., Miller B. (1997), Stress Fluctuations for Sheared 3D Granular Materials, *Proc. Powder and Grains* (Behringer and Jenkins, eds.), Balkema, 333–336.

Böhrnsen J. U. (2002), *Dynamisches Verhalten von Schüttgütern beim Entleeren aus Silos*, PhD Thesis, University of Braunschweig, Germany.

Borst R. de (1991), Simulation of Strain Localization: a Reappraisal of the Cosserat Continuum, *Engng. Computations*, 8, 317–332.

Borst R. de, Mühlhaus H. B., Pamin J., Sluys L. Y. (1992), Computational Modelling of Localization of Deformation, *Proc. of the 3rd Int. Conf. Comp. Plasticity* (D. R. J. Owen, E. Onate, E. Hinton, eds.), Pineridge Press, Swansea, 483–508.

Bransby P. L. (1968), *Stress and Strain in Sand Caused by Rotation of a Model Wall*, PhD Thesis, University of Cambridge.

Bransby P. L., Milligan G. W. E. (1975), Soil Deformations Near Cantilever Sheet Pile Walls, *Géotechnique*, 25, 2, 175–195.

Brinkgreve R. (1994), *Geomaterial Models and Numerical Analysis of Softening*, PhD Thesis, Delft University.

Caquot A., Kerisel J. (1948), *Tables for the Calculation of Passive Pressures, Active Pressures and Bearing Capacity of Foundations*, Gauthier-Villars, Paris.

Christian J. T., Hagmann A. J., Marr W. A. (1977), Incremental Plasticity Analysis of Frictional Soils, *Int. J. Num. Anal. Meth. Geomech.*, 1, 343–375.

Coulomb C. A. (1775), *Essai Sur une Application*, Science et Industrie, Paris.

Darwin G. H. (1883), On the Horizontal Thrust of a Mass of Sand, *Proc. Inst. Civ. Eng.*, 71, 350–378.

Dembicki E. (1979), *Active, Passive Earth Pressure and Bearing Capacity*, Arkady, Warszawa (in Polish).

Desrues J., Hammad W. (1989), Shear Banding Dependency on Mean Pressure Level in Sand, *Proc. Int. Workshop on Numerical Methods for Localization and Bifurcation of Granular Bodies*, (E. Dembicki et al, eds.), Gdańsk, Poland, 57–67.

Desrues J., Chambon R., Mokni M., Mazerolle F. (1996), Void Ratio Evolution Inside Shear Bands in Triaxial Sand Specimens Studied by Computed Tomography, *Géotechnique*, 46, 3, 529–546.

Ehlers W., Graf T. (2003), Adaptive Computation of Localization Phenomena in Geotechnical Applications, In: *Bifurcations and Instabilities in Geomechanics* (J. Labuz and A. Drescher, eds), Swets and Zeitlinger, 247–262.

Ehlers W., Ramm E., Diebels S., D'Addetta G. A. (2003), From Particle Ensembles to Cosserat Continua: Homogenisation of Contact Forces Towards Stresses and Couple Stresses, *Int. J. Solids and Structures*, 40, 6681–6702.

Fourie A. B., Potts D. M. (1989), Comparison of Finite Element and Limiting Equilibrium Analyses for an Embedded Cantilever Retaining Wall, *Géotechnique*, 39, 2, 175–188.

Geng J., Hartley R. R., Howell D., Behringer R. P., Reydellet G., Clement E. (2003), Fluctuations and Instabilities in Granular Materials, In: *Bifurcations and Instabilities in Geomechanics* (J. Labuz and A. Drescher, eds.), Swets and Zeitlinger, 79–108.

Groen A. E. (1997), *Three-Dimensional Elasto-Plastic Analysis of Soils,*. PhD Thesis, Delft University.

Gudehus G. (1978), Engineering Approximations for Some Stability Problems in Geomechanics, *Advances in Analysis of Geotechnical Instabilities*, University of Waterloo Press, 13, 1–24.

Gudehus G. (1986), Einige Beiträge der Bodenmechanik zur Entstehung und Auswirkung von Diskontinuitäten, *Felsbau*, 4, 190–195.

Gudehus G., Schwing E. (1986), Standsicherheit Historischer Stützwände, *Internal Report of the Institute of Soil and Rock Mechanics*, University Karlsruhe.

Gudehus G. (1996a), A Comprehensive Constitutive Equation for Granular Materials, *Soils and Foundations*, 36, 1, 1–12.

Gudehus G. (1996b), *Erddruckermittlung*, Grundbautaschenbuch, Teil 1, Ernst und Sohn.

Gudehus G., Nübel K. (2004), Evolution of Shear Bands in Sand., *Géotechnique*, 54(3), 187–201.

Herle I. (1998), A Relation between Parameters of a Hypoplastic Constitutive Model and Grain Properties, In: *Localisation and Bifurcation Theory for Soils and Rocks in Gifu*, ed.: T. Adachi, F. Oka, A. Yashima, Balkema, 91–99.

Herle I., Gudehus G. (1999), Determination of Parameters of a Hypoplastic Constitutive Model from Properties of Grain Assemblies, *Mechanics of Cohesive-Frictional Materials*, 4, 5, 461–486.

Hicks M. A., Yap T. Y., Bakar A. A. (2001), Adaptive and Fixed Mesh Study of Localisation in a Strain-Softening Soil, In: *Bifurcation and Localisation Theory in Geomechanics* (H. B. Mühlhaus, A. Dyskin and E. Pasternak, eds.), Balkema, 147–155.

Houlsby G. T., Wroth C. P. (1982), Direct Solution of Plasticity Problems in Soils by the Method of Characteristics, *Proc. 4th Int. Conf. on Num. Meth. in Geomech.*, Edmonton, Canada, 1059–1071.

Huang W., Nübel K., Bauer E. (2002), A Polar Extension of Hypoplastic Model for Granular Material with Shear Localization, *Mechanics of Materials*, 34, 563–576.

James R. G. (1965), *Stress and Strain Fields in Sand,* PhD Thesis, University of Cambridge.

James R. G., Bransby P. L. (1971), A Velocity Field for Some Passive Earth Pressure Problems, *Géotechnique,* 21, 1, 61–83.

Leśniewska D. (2000), *Analysis of Shear Band Pattern Formation in Soil*, Habilitation, Institute of Hydro-Engineering of the Polish Academy of Sciences, Gdańsk, Poland.

Leśniewska D., Mróz Z. (2000), Limit Equilibrium Approach to Study the Evolution of Shear Band Systems in Soil, *Géotechnique*, 50, 389–403.

Leśniewska D., Mróz Z. (2001), Study of Evolution of Shear Band Systems in Sand Retained by Flexible Wall, *Int. J. Numer. Anal. Meth. Geomech.,* 25, 909–932.

Leśniewska D., Mróz Z. (2003), Shear Bands in Soil Deformation Processes, In: *Bifurcations and Instabilities in Geomechanics* (J. Labuz and A. Drescher, eds.), Swets and Zeitlinger, 109–119.

Lord J. A. (1969), *Stress and Strains in an Earth Pressure Problem*, PhD Thesis, University of Cambridge.

Lucia J. B. A. (1966), *Passive Earth Pressure and Failure in Sand*, Research Report, University of Cambridge.

Maier T. (2002), *Numerische Modellierung der Entfestigung im Rahmen der Hypoplastizität*, PhD Thesis, Dortmund University, Germany.

Marcher T., Vermeer P. A. (2001), Macromodelling of Softening in Non-Cohesive Soils, In: *Continuous and Discontinuous Modelling of Cohesive-Frictional Materials* (P. A. Vermeer et al, eds.), Springer-Verlag, 89–110.

May J. (1967), *A Pilot Project on the Cutting of Soils,* Research Report, University of Cambridge.

Milligan G. W. E. (1974), The Behaviour of Rigid and Flexible Retaining Walls in Sand, *Géotechnique*, 26, 3, 473–494.

Milligan G. W. E. (1983), Soil Deformations Near Anchored Sheet-Pile Walls, *Géotechnique*, 33, 1, 41–55.

Mühlhaus H. B. (1989), Application of Cosserat Theory in Numerical Solutions of Limit Load Problems, *Ing. Arch.*, 59, 124–137.

Mühlhaus, H. B. (1990), Continuum Models for Layered and Blocky Rock, In: *Comprehensive Rock Engineering* (Hudson, J. A., Fairhurst, Ch., eds.), Pergamon Press, 2, 209–231.

Nakai T. (1985), Analysis of Earth Pressure Problems Considering the Influence of Wall Friction and Wall Deflection, *Proc. Int. Conf. Num. Meth. Geomech.*, Nagoya, 765–772.

Negre R. (1959), *Sur Une Methode Approchee de la Repatition des Equilibre Limite des Massifs Plans a Faible Frottement Interne*, C. R. A. S., Paris, 3118–3120.

Niemunis A., Herle I. (1997), Hypoplastic Model for Cohesionless Soils with Elastic Strain Range, *Mechanics of Cohesive-Frictional Materials*, 2, 279–299.

Nübel K., Karcher Ch. (1998), FE Simulations of Granular Material with a Given Frequency Distribution of Voids as Initial Condition, *Granular Matter*, 1, 3, 105–112.

Nübel K. (2002), Experimental and Numerical Investigation of Shear Localisation in Granular Materials, *Publication Series of the Institute of Soil and Rock Mechanics, University Karlsruhe,* 62.

Nübel K., Huang W. X. (2004), A Study of Localized Deformation Pattern in Granular Media, *Comp. Method Appl. M.*, 193, 2719–2743.

Oda M., Konishi J., Nemat-Nasser S. (1982), Experimental Micromechanical Evaluation of Strength of Granular Materials, Effects of Particle Rolling, *Mechanics of Materials*, North-Holland Publishing Comp., 1, 269–283.

Oda M. (1993), Micro-fabric and Couple Stress in Shear Bands of Granular Materials, In: *Powders and Grains* (C. Thornton ed.), Rotterdam, Balkema, 161–167.

Oda M., Kazama H. (1998), Micro-Structure of Shear Band and its Relation to the Mechanism of Dilatancy and Failure of Granular Soils, *Géotechnique*, 48, 465–481.

Pamin J. (1994), *Gradient-Dependent Plasticity in Numerical Simulation of Localisation Phenomena*, PhD Thesis, Delft University.

Pasternak E., Mühlhaus H.-B. (2001), Cosserat Continuum Modelling of Granulate Materials, In: *Computational Mechanics – New Frontiers for New Millennium* (Valliappan S. and N. Khalili, eds.), Elsevier Science, 1189–1194.

Potts D. M., Fourie A. B. (1984), The Behaviour of a Propped Retaining Wall: Results of a Numerical Experiment, *Géotechnique,* 34, 3, 383–404.

Roscoe K. H. (1970), The Influence of Strains in Soil Mechanics, *Géotechnique*, 20, 2, 129–170.

Schäfer H. (1962), Versuch einer Elastizitätstheorie des Zweidimensionalen Ebenen Cosserat-Kontinuums, *Miszellaneen der Angewandten Mechanik*, Festschrift Tolmien, W., Berlin, Akademie-Verlag.

Simpson B. (1972), *The Use of Finite Element Technique in Soil Mechanics with Particular Reference to Deformation in Plane Strain,* PhD Thesis, University of Cambridge.

Simpson B., Wroth C. P. (1974), Finite Element Computations for a Model Retaining Wall in Sand, *Proc. Int. Conf. on Num. Meth. in Geomech*, (Z. Eisenstein, ed.), Edmonton, 1982, 85–93.

Sluys L. J. (1992), *Wave Propagation, Localisation and Dispersion in Softening Solids*, PhD Thesis, Delft University of Technology.

Smith I. (1972), *Stress and Strain in a Sand Mass Adjacent to a Model Wall*, PhD Thesis, University of Cambridge.

Sokolovski V. V. (1965), *Statics of Granular Media*,. Pergamon Press.

Steinmann P. (1995), Theory and Numerics of Ductile Micropolar Elastoplastic Damage, *Int. J. for Num. Meth. in Engng.*, 38, 583–606.

Szczepiński W. (1974), *Limit States and Kinematics of Granular Materials* (in Polish), PWN Warszawa.

Tatsuoka F., Okahara M., Tanaka T., Tani K., Morimoto T., Siddiquee M. S. (1991), Progressive Failure and Particle Size Effect in Bearing Capacity of Footing on Sand, *Proc. of the ASCE Geotechnical Engineering Congress,* 27, 2, 788–802.

Tatsuoka F., Siddiquee M. S., Yoshida T., Park C. S., Kamegai Y., Goto S., Kohata Y. (1994), Testing Methods and Results of Element Tests and Testing Conditions of Plane Strain Model Bearing Capacity Tests using Air-Dried Dense Silver Buzzard Sand, *Internal Report of the University of Tokyo*, 1–129.

Tatsuoka F., Goto S., Tanaka T., Tani K., Kimura Y. (1997), Particle Size Effects on Bearing Capacity of Footing on Granular Material, In: *Deformation and Progressive Failure in Geomechanics*, (A. Asaoka, T. Adachi, and F. Oka, eds.), Pergamon, 133–139.

Tejchman J. (1989), Scherzonenbildung und Verspannungseffekte in Granulaten unter Berücksichtigung von Korndrehungen, *Publication Series of the Institute of Soil and Rock Mechanics, University Karlsruhe,* 117, 1–236.

Tejchman J., Wu W. (1993), Numerical Study on Shear Band Patterning in a Cosserat Continuum, *Acta Mechanica*, 99, 61–74.

Tejchman J. (1997), Modelling of Shear Localisation and Autogeneous Dynamic Effects in Granular Bodies, *Publication Series of the Institute of Soil and Rock Mechanics*, University Karlsruhe, 140, 1–353.

Tejchman J. (1998), Numerical Simulation of Filling in Silos with a Polar Hypoplastic Constitutive Law, *Powder Technology*, 96, 227–239.

Tejchman J., Herle I., Wehr J. (1999), FE-Studies on the Influence of Initial Void Ratio, Pressure Level and Mean Grain Diameter on Shear Localisation, *Int. J. Num. Anal. Meth. Geomech.*, 23, 2045–2074.

Tejchman J., Herle I. (1999), A Class "A" Prediction of the Bearing Capacity of Plane Strain Footings on Granular Material, *Soils and Foundations*, 39, 5, 47–60.

Tejchman J. (2000), Behaviour of Granular Bodies in Induced Shear Zones, *Granular Matter*, 2, 2, 77–96.

Tejchman J., Gudehus G. (2001), Shearing of a Narrow Granular Strip with Polar Quantities, *Int. J. Num. and Anal. Methods in Geomechanics*, 25, 1–28.

Tejchman J., Dembicki E. (2001), Numerical Analysis of Active and Passive Pressure of Cohesionless Soil, *Inżynieria Morska i Geotechnika,* 6, 365–368 (in Polish).

Tejchman J. (2002a), Patterns of Shear Zones in Granular Materials within a Polar Hypoplastic Continuum, *Acta Mechanica*, 155, 1–2, 71–95.

Tejchman J. (2002b), Evolution of Shear Localisation at Earth Pressure Problems of a Retaining Wall, *Task Quarterly*, Gdańsk University of Technology, 6, 3, 387–410.

Tejchman J. (2002c), Effects of Wall Inclinations and Sall Imperfections on Pressures during Silo Flow in Silos, *Kona*, 20, 1–8.

Tejchman J. (2003), A Non-Local Hypoplastic Constitutive Law to Describe Shear Localisation in Granular Bodies, *Archives of Hydro-Engineering and Environmental Mechanics,* 50, 4, 229–250.

Tejchman J., Bauer E. (2004), Effect of Cyclic Shearing on Shear Localization in Granular Bodies, *Granular Matter*, 5, 201–212.

Tejchman J. (2004a), Comparative FE-Studies of Shear Localizations in Granular Bodies within a Polar and Non-Local Hypoplasticity, *Mechanics Research Communications,* 3, 1, 341–354.

Tejchman J. (2004b), Effect of Heterogeneity on Shear Zone Formation During Plane Strain Compression, *Archives of Hydro-Engineering and Environmental Mechanics,* Vol. LI, 2, 149–183.

Tejchman J. (2004c), Simulations of Shear Localization with Gradient-Enhanced Hypoplasticity, *Archives of Hydro-Engineering and Environmental Mechanics,* Vol. LI, 3, 243–265.

Terzaghi K. (1951), *Mecanique Theorique des Sols*, Dunod., Paris.

Uesugi M., Kishida H., Tsubakihara Y. (1988), Behaviour of Sand Particles in Sand-Steel Friction, *Soils and Foundations*, 28, 1, 107–118.

Vardoulakis I. (1980), Shear Band Inclination and Shear Modulus in Biaxial Tests, *Int. J. Num. Anal. Meth. Geomech.*, 4, 103–119.

Vermeer P. A., van Langen H. (1989), Soil Collapse Computations with Finite Elements, *Ing. Arch.*, 59, 221–236.

Wang C. C. (1970), A New Representation Theorem for Isotropic Functions, *J. Rat. Mech. Anal.*, 36, 166–223.

Wang Y. Z. (2000), Distribution of Earth Pressure on a Retaining Wall, *Géotechnique,* 50, 1, 83–88.

Wehr J., Tejchman J. (1999), Sand Anchors in Rock and Granular Soils – Experiments and a Polar Hypoplastic Approach, In: *Proc. World Civil and Environmental Engineering Conference*, Thailand (eds. A.S. Balasubramaniam et al), 2, VII 1–10.

Wolffersdorff P. A. von (1996), A Hypoplastic Relation for Granular Materials with a Predefined Limit State Surface, *Mechanics Cohesive-Frictional Materials*, 1, 251–271.

Wu W., Niemunis A. (1996), Failure Criterion, Flow Rule and Dissipation Function Derived from Hypoplasticity, *Mechanics of Cohesive-Frictional Materials*, 1, 145–163.

Zaimi S. A. (1998), *Modelisation de l'Coulement des Charges dans le Haut Fourneau*, PhD Thesis, Ecole Centrale Paris, France.

Zervos A., Papanastasiou P., Vardoulakis I. (2001), A Finite Element Displacement Formulation for Gradient Elastoplasticity, In: *Bifurcation and Localisation Theory in Geomechanics* (H. B. Mühlhaus, A. Dyskin and E. Pasternak, eds.), Balkema, 177–187.

Ziegler M. (1986), *Berechnung des Verschiebungsabhängigen Erddruckes in Sand*, PhD Thesis, Institute for Soil and Rock Mechanics, Karlsruhe University.